Multi-Criteria Optimization of Pressure Screen Systems in Paper Recycling – Balancing Quality, Yield, Energy Consumption and System Complexity

Tim M. Müller✉[1], Lena C. Altherr[1], Marja Ahola[2], Samuel Schabel[2], and Peter F. Pelz[1]

[1] Chair of Fluid Systems, Technische Universität Darmstadt, Darmstadt, Germany.
tim.mueller@fst.tu-darmstadt.de,
WWW: www.fst.tu-darmstadt.de
[2] Chair of Paper Technology and Mechanical Process Engineering, Technische Universität Darmstadt, Darmstadt, Germany.
WWW: www.pmv.tu-darmstadt.de

Abstract. The paper industry is the industry with the third highest energy consumption in the European Union. Using recycled paper instead of fresh fibers for papermaking is less energy consuming and saves resources. However, adhesive contaminants in recycled paper are particularly problematic since they reduce the quality of the resulting paper-product. To remove as many contaminants and at the same time obtain as many valuable fibres as possible, fine screening systems, consisting of multiple interconnected pressure screens, are used. Choosing the best configuration is a non-trivial task: The screens can be interconnected in several ways, and suitable screen designs as well as operational parameters have to be selected. Additionally, one has to face conflicting objectives. In this paper, we present an approach for the multi-criteria optimization of pressure screen systems based on Mixed-Integer Nonlinear Programming. We specifically focus on a clear representation of the trade-off between different objectives.

Keywords: Multi-Criteria Optimization, Mixed-Integer Nonlinear Problem, SCIP, Paper Recycling, Screening Systems, Process Engineering, Graphical User Interface, Decision-Support.

1 Introduction

Despite a trend to paperless offices, the demand for paper products is still slightly rising: In the European Union 82.000 tons of paper were consumed in 2015 [16]. The paper industry is – with an annual energy consumption in 2015 of 387 TWh – the industry branch with the third highest energy consumption in the European Union [4]. To save resources, more than half of the paper is made out of paper for recycling which is less energy consuming compared to the usage of fresh fibres [7]. To produce new paper from heterogeneous recycled paper,

pre-processing is required to remove as many contaminants as possible. Adhesive contaminants, so-called stickies, are particularly problematic: They lead to problems during the papermaking process, are difficult to remove and reduce the quality of the resulting paper-product. The paper is first disintegrated resulting in a suspension containing water, fibres and contaminants. Then, the suspension passes several stages of separation. The fine screening system, consisting of multiple interconnected pressure screens, is used to separate stickies from fibres.

Choosing the best configuration of such a multi-stage screening system is a non-trivial task: The screens can be interconnected in several ways and suitable single screens as well as operational parameters have to be selected. Additionally, one has to find a trade-off between conflicting objectives: The loss of valuable fibres should be as low as possible, while at the same time guaranteeing a high quality of the end product by removing as many stickies as possible.

In the literature, various studies are dealing with the design and analysis of pressure screen systems, e.g. [5, 13, 17]. However, in industrial settings, the planning and operation of such systems is still based on rules of thumb and on expert knowledge. Remaining challenge is to bridge the gap between mathematical expert knowledge and its application in real world engineering settings.

In this work, our goal is to extend the model in [5] and to faciliate access to our optimization approach for practitioners. Besides maximizing quality and fibre yield, we deal with the additional objectives of minimizing resource-consumption and complexity of the system. To transfer our results to industrial settings, we present a software tool with a problem-specific graphical user interface (GUI). It allows for a simple formulation and an easy adaptation of the optimization model to individual constraints such as existing infrastructure, as well as for a clear graphical representation of the results of the multi-criteria optimization.

2 Technical Application

When modelling the fine screening process, some assumptions have to be made and the scope of the model has to be defined. Fig. 1, left shows a single pressure screen and its abstraction in the model. The suspension flows into the screen at the feed. Inside, slotted or holed screen baskets are used to retain as much stickies as possible. They accumulate in the so called reject flow, which has a lower quality compared to the feed. The fibres should pass the basket and accumulate in the high quality accept flow. A rotor moves close to the basket surface and generates a suction pulse to prevent blinding of the screen apertures.

To increase the performance, several screens are interconnected to multi-stage screening systems, cf. Fig. 1 right. The accept or reject of one screen is then fed into another screen before it enters the total accept or reject of the system.

The input of the screening system is a suspension consisting of water W, fibres F and stickies S which constitute the set of components $K = \{\mathrm{F}, \mathrm{S}, \mathrm{W}\}$. Each of those components is modelled as a separate flow. Only the screens of the system, their connections and the system input, accept and reject are modelled. Other components, such as pumps, tanks or valves, are neglected. We derive

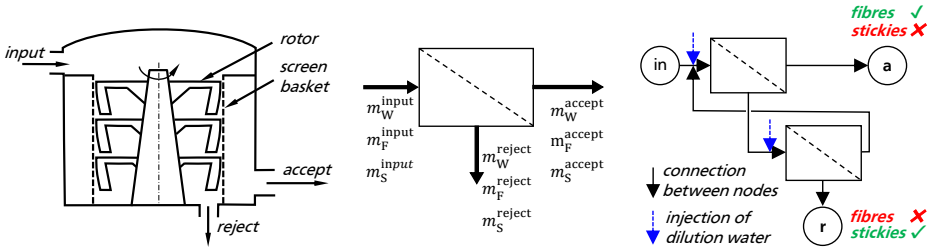

Fig. 1. *Left:* Industrial single pressure screen. *Middle:* Abstracted pressure screen with definition of the component's flow. *Right:* Exemplary system using two screens and cascade feedback topology. It is possible to inject dilution water before each screen. Fibres should accumulate in the system accept a and stickies in the system reject r.

balance equations for the water volume flow m_{W}, the fibre mass flow m_{F} and the sticky surface area flow m_{S} where we assume a steady state. Fig.1, middle shows the abstracted pressure screen and the definition of the respective flows. We apply the widely established plug-flow model [14] to describe the separation of the pressure screens. Moreover, mass conservation holds for all components. By neglecting its compressibility, one can assume volume conservation for the water. By neglecting agglomeration and disintegration of stickies, one can assume conservation of the stickies' total area flow. This leads to:

$$m_k^{\mathrm{feed}} = m_k^{\mathrm{accept}} + m_k^{\mathrm{reject}} \quad \forall k \in K. \tag{1}$$

Furthermore, the separation between accept and reject of each component is specified. The volumetric reject ratio r describes the separation of the water volume flow into accept and reject, cf. Eq. 2. It is an adjustable operational parameter. According to the plug flow model, the separation of fibres and stickies depends on r and on the passage ratio P_k with $k \in \{F, S\}$, see Eq. 3. Here, P_k denotes the probability of a single fibre or sticky to pass the screen basket.

$$\frac{m_{\mathrm{W}}^{\mathrm{accept}}}{m_{\mathrm{W}}^{\mathrm{reject}}} = r \tag{2}$$

$$\frac{m_k^{\mathrm{accept}}}{m_k^{\mathrm{reject}}} = r^{p_k} \quad \forall k \in \{F, S\} \tag{3}$$

The passage ratios P_{F} and P_{S} of fibres and stickies are strongly influenced by the design of the screen and are moreover dependent on each other. E.g., a large slot width of the basket causes a high passage ratio of fibres, as well as of stickies. Experimental data from [1] show that this relation is widely unique and that changes of different design parameters finally lead to the same effect: Either P_{F} and P_{S} are both decreased or both increased. Fig. 2 shows measured passage ratios of screens with different designs, as well as an exponential function fitted to this data, where the coefficients are derived by a least square approximation:

$$P_{\mathrm{S}} = 0.005901 \cdot \exp(5.132\, P_{\mathrm{F}}) \tag{4}$$

This dependency causes a conflict, since a high passage ratio of the fibres (yielding low fibre loss) as well as a low passage ratio of the stickies (yielding high quality) are desired. Thus, a trade-off must be made when selecting the screens.

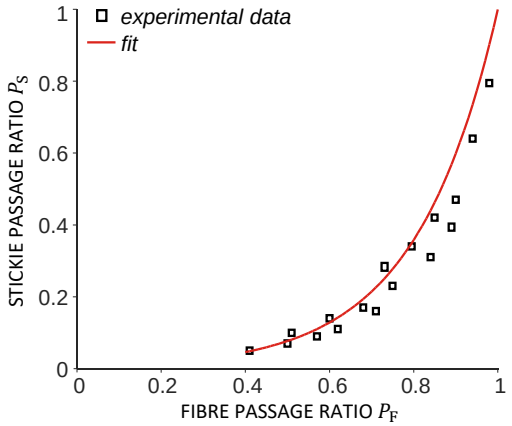

Fig. 2. Measured fibre and sticky passage ratio of pressure screens with different design [1] and fitted relation between them.

3 Optimization Problem

In this section, the optimization problem is presented. First, the parameters and variables, as well as the performance indicators are introduced. Afterwards, the MINLP is presented (Eqs. 9 – 35).

3.1 Parameters and Variables

Variables are denoted by small letters (see Tab. 1). Sets (see Tab. 2) and parameters (see Tab. 3) are denoted by capital letters or greek letters. The nomenclature is inspired by [5].

The system topology is modelled by two directed graphs G^λ, one for the accept connections ($\lambda = \text{accept}$), and one for the reject connections ($\lambda = \text{reject}$). The nodes of these graphs are the screens $Sc = \{sc_1, ..., sc_{N_{sc}}\}$, the system input in, the system total accept a and total reject r. Nodes with a possible outgoing connection (sources) are the output nodes $V^+ = Sc \cup \{in\}$ and nodes with a possible incoming connection (sinks) are the feed nodes $V^- = Sc \cup \{a, r\}$. To indicate which accept and reject connections are chosen, binary adjacency matrices $t^\lambda_{i,j}$ of the two graphs G^λ are introduced. They describe whether a connection from the accept/reject of node $i \in V^+$ to the input of node $j \in V^-$ exists ($t^\lambda_{i,j} = 1$) or not ($t^\lambda_{i,j} = 0$). Respectively, matrices $m^\lambda_{i,j,k}$ are introduced, denoting the flow of component $k \in K$ on edge (i, j).

Table 1. Decision Variables.

Variable	Domain	Description
$t^{\lambda}_{i,j}$	$\{0,1\}$	Connection indicator between nodes i and j, $\lambda \in \Lambda$.
$m^{\text{feed}}_{j,k}$	$\mathbb{R}^+_0$	Feed flow of component $k \in K$ into node $j \in V^-$.
$m^{\lambda}_{i,j,k}$	$\mathbb{R}^+_0$	Flow of component $k \in K$ between accept or reject of node $i \in V^+$ and feed of node $j \in V^-$, $\lambda \in \Lambda$.
$m^{\text{dil}}_{i,\text{W}}$	$\mathbb{R}^+_0$	Flow of dilution water into node $i \in V^+$.
r_{sc}	$[0.1, 0.8]$	Volumetric reject ratio of screen $sc \in Sc$.
$p_{sc,k}$	$\mathbb{R}^+_0$	Passage ratio of screen $sc \in Sc$ for component $k \in \{\text{F}, \text{S}\}$.
$b_{sc,d}$	$\{0,1\}$	Indicator for chosen design $d \in D$ for screen $sc \in$ Sc.
i_l	$\mathbb{R}^+_0$	Performance indicators with $l \in \{\text{W}, \text{F}, \text{S}, \text{E}\}$.

Table 2. Sets.

Set	Description
Sc	Set of all screens.
$\{in, a, r\}$	Set of system input, accept and reject node.
V^+	Set of nodes with a possible outgoing connection $V^+ = Sc \cup \{\text{in}\}$.
V^-	Set of nodes with a possible incoming connection $V^- = Sc \cup \{\text{a}, \text{r}\}$.
K	Set of modelled components $\{\text{F}, \text{S}, \text{W}\}$ (Fibres, Stickies, Water).
D	Set of possible screen designs.
Λ	Index set $\{\text{accept}, \text{reject}\}$.

Table 3. Parameters.

Parameter	Range	Description
α_l	$[0,1]$	Weight of performance indicator l.
$I^{\max}_l$	$\mathbb{R}^+_0$	Upper bound of performance indicators with $l \in \{\text{W}, \text{F}, \text{S}, \text{E}\}$.
N_{sc}	$\mathbb{N}^+_0$	Maximum number of screens used in the system.
M^{input}_k	$\mathbb{R}^+_0$	Total input flow of component $k \in K$ into the system.
$M^{\max}_k$	$\mathbb{R}^+_0$	Maximum pipe capacity of component $k \in K$.
$P^{\text{pre}}_{k,d}$	$\mathbb{R}^+_0$	Passage ratio of fibres and stickies ($k \in K$) for design $d \in D$.
$C^{\max}$	0.04	Maximum consistency (ratio of fibre mass to water).
$T^{\lambda}_{i,j}$	$\{0,1\}$	Partly given topology indicating connection between i and j.

3.2 Performance Indicators

We introduce performance indicators for each objective considered. All indicators are chosen so that a low value indicates a high performance. This simplifies the interpretation of the results.

Fibre loss: Since fibres are the valuable product of the process, the fibre loss should be as low as possible. The loss is quantified by the amount of fibres flowing into in the system reject $m^{\text{feed}}_{\text{r,F}}$ in relation to the system input of fibres $M^{\text{input}}_{\text{F}}$:

$$i_{\text{F}} \coloneqq \frac{m^{\text{feed}}_{\text{r,F}}}{M^{\text{input}}_{\text{F}}}. \tag{5}$$

Sticky load: Stickies reduce the quality of the product and should be avoided in the accept. The sticky load is defined as the amount of stickies flowing into the system accept $m_{\mathrm{a,S}}^{\mathrm{feed}}$ in relation to the system input of stickies $M_{\mathrm{S}}^{\mathrm{input}}$:

$$i_{\mathrm{S}} \coloneqq \frac{m_{\mathrm{a,S}}^{\mathrm{feed}}}{M_{\mathrm{S}}^{\mathrm{input}}}. \tag{6}$$

Energy consumption: The energy consumption is determined mainly by the drive power for the screen rotors and the power to pump the suspension. Since no sophisticated generic models are available, an indirect indicator is used. As shown in various studies, the primarily determining factor is the volume flow through a screen [2, 12]. Thus, the energy consumption is quantified by the volume flow through all screens in relation to the input volume flow $M_{\mathrm{W}}^{\mathrm{input}}$:

$$i_{\mathrm{E}} \coloneqq \frac{\sum_{sc \in Sc} m_{sc,\mathrm{W}}^{\mathrm{feed}}}{M_{\mathrm{W}}^{\mathrm{input}}}. \tag{7}$$

Furthermore, this indicator represents the machine expenditure. For higher relative flows, larger screens are necessary, tending to result in higher investment and operating costs.

Water consumption: Dilution water is used to lower the suspension's consistency (ratio of fibre mass flow to volume flow). Even if water is partially reused, a low consumption is preferred, since its treatment for reuse requires additional effort and cost. Water consumption is defined as:

$$i_{\mathrm{W}} = \frac{\sum_{sc \in Sc} m_{sc,\mathrm{W}}^{\mathrm{dil}}}{M_{\mathrm{W}}^{\mathrm{input}}}. \tag{8}$$

Complexity: The system's complexity is determined by its number of screens N_{sc}. More screens increase the system's costs and error-proneness.

3.3 Mixed-Integer Nonlinear Program

The optimization problem is given by Eqs. 9 – 35. We use the weighted sum method and combine four performance indicators to one objective function, cf. Eq. 9. By setting α_i, $i \in \{1, 2, 3, 4\}$, the weight of the indicators can be adjusted. Each indicator is bounded, cf. Eq. 10 – 13. The number of screens used in the system is restricted by N_{sc}.

The fibre and sticky inflow of each screen and of system accept and reject are defined in Eq. 14. By injecting dilution water the consistency can be lowered and blinding of the screens can be avoided. Thus, dilution water has to be considered for calculating the water inflow in Eq. 15. Since a dilution into the accept or reject node is useless, it is omitted in Eq. 16. The conservation laws for each screen, cf. Eq. 1, are modelled in Eq. 17. The separation according to the plug flow model, cf. Eq. 3, is guaranteed by Eq 18. The volumetric reject rate is calculated in Eq. 19. The bigM formulation in Eq. 20 models that flow between two nodes is only possible if there is a connection between them.

Eqs. 21 – 23 model the selection of a suitable screen. Out of a set of predefined screen-designs with specific sticky and fibre passage ratios $P^{\text{pre}}_{k,d}$, exactly one design d has to be chosen for each screen sc. Note that by choosing from a set of discrete designs, we do not have to integrate the nonlinearity of Eq. 4 into our model, but additional binary variables $b_{sc,d}$ are introduced. This approach considerably speeds up the optimization if not too many designs are considered.

To avoid blinding of the screen basket, the consistency of the reject has to be limited according to the maximum allowed consistency $C^{\max}$, see Eq. 24. Eq. 25 limits the number of outgoing connections of a single node. Connections from the input are defined as accept connections. Thus, reject connections from the input have to be excluded (Eq. 26). All the system input flow has to be distributed to the screens via accept connections, see Eq. 27.

To speed up the optimization, obviously non-optimal topologies are omitted: No accept connections to the system reject and no reject connections to the system accept are allowed, cf. Eqs. 28. Back flow into the same screen is not permitted (Eq. 29), and accept and reject connection of one screen must not enter the same node (Eqs. 30, 31). Also, permutations are excluded: The input has to be connected to the first screen (Eq. 32). Accept connections from screen sc_i to screen sc_{i+2} are forbidden (Eq. 33). Also reject connections between those screens, if there is no accept connection from screen sc_i to screen sc_{i+1} (Eq. 34). This guarantees that all screens are connected in ascending order.

All of the connections defined in $T^{\lambda}_{i,j}$ have to be used (Eq. 35). Thus, a part of the topology is predetermined and one can account for an existing infrastructure.

$$\min \qquad \alpha_1\, i_{\text{F}} + \alpha_2\, i_{\text{S}} + \alpha_3\, i_{\text{E}} + \alpha_4\, i_{\text{W}} \tag{9}$$

subject to

$$i_{\text{F}} = \frac{m^{\text{feed}}_{\text{r,F}}}{M^{\text{input}}_{\text{F}}} \leq I^{\max}_{\text{F}} \tag{10}$$

$$i_{\text{S}} = \frac{m^{\text{feed}}_{\text{a,S}}}{M^{\text{input}}_{\text{S}}} \leq I^{\max}_{\text{S}} \tag{11}$$

$$i_{\text{E}} = \frac{\sum_{sc \in Sc} m^{\text{feed}}_{sc,\text{W}}}{M^{\text{input}}_{\text{W}}} \leq I^{\max}_{\text{E}} \tag{12}$$

$$i_{\text{W}} = \frac{\sum_{sc \in Sc} m^{\text{dil}}_{sc,\text{W}}}{M^{\text{input}}_{\text{W}}} \leq I^{\max}_{\text{W}} \tag{13}$$

$$m^{\text{feed}}_{j,k} = \sum\nolimits_{i \in V^+, \lambda \in \Lambda} m^{\lambda}_{i,j,k} \qquad \forall j \in V^-, k \in \{F, S\} \tag{14}$$

$$m^{\text{feed}}_{j,\text{W}} = \sum\nolimits_{i \in V^+, \lambda \in \Lambda} m^{\lambda}_{i,j,\text{W}} + m^{\text{dil}}_{j,\text{W}} \qquad \forall j \in V^- \tag{15}$$

$$m^{\text{dil}}_{\text{a,W}} = m^{\text{dil}}_{\text{r,W}} = 0 \tag{16}$$

$$m^{\text{feed}}_{sc,k} = \sum\nolimits_{j \in V^-, \lambda \in \Lambda} m^{\lambda}_{sc,j,k} \qquad \forall sc \in Sc, k \in K \tag{17}$$

$$\sum\nolimits_{j \in V^-} m^{\text{reject}}_{sc,j,k} = m^{\text{feed}}_{sc,k}\, r^{p_{sc,k}}_{sc} \qquad \forall sc \in Sc, k \in \{F, S\} \tag{18}$$

$$\sum\nolimits_{j\in V^-} m^{\text{reject}}_{i,j,\text{W}} = m^{\text{feed}}_{s,\text{W}} \cdot r_i \quad \forall sc \in Sc \tag{19}$$

$$0 \leq m^{\lambda}_{i,j,k} \leq M^{\max}_{k} \cdot t^{\lambda}_{i,j} \quad \forall i \in V^+, j \in V^-, k \in K \tag{20}$$

$$p_{sc,k} - P^{\text{pre}}_{k,d} \leq (1 - b_{sc,d}) \quad \forall sc \in Sc, d \in D, k \in \{F, S\} \tag{21}$$

$$p_{sc,k} - P^{\text{pre}}_{k,d} \geq -(1 - b_{sc,d}) \quad \forall sc \in Sc, d \in D, k \in \{F, S\} \tag{22}$$

$$\sum\nolimits_{d\in D} b_{sc,d} = 1 \quad \forall sc \in Sc \tag{23}$$

$$\sum\nolimits_{j\in V^-} m^{\text{reject}}_{sc,j,F} \leq C^{\max} \sum\nolimits_{j\in V^-} m^{\text{reject}}_{sc,j,\text{W}} \quad \forall sc \in Sc \tag{24}$$

$$\sum\nolimits_{j\in V^-} t^{\lambda}_{i,j} \leq 1 \quad \forall i \in V^+, \lambda \in \Lambda \tag{25}$$

$$\sum\nolimits_{j\in V^-} t^{\text{reject}}_{\text{in},j} = 0 \tag{26}$$

$$\sum\nolimits_{sc\in Sc} m^{\text{accept}}_{\text{in},sc,k} = M^{\text{input}}_{k} \quad \forall k \in K \tag{27}$$

$$\sum\nolimits_{i\in V^+} t^{\text{accept}}_{i,\text{r}} = \sum\nolimits_{i\in V^+} t^{\text{reject}}_{i,\text{a}} = 0 \tag{28}$$

$$t^{\lambda}_{sc,sc} = 0 \quad \forall sc \in Sc, \lambda \in \Lambda \tag{29}$$

$$t^{\text{reject}}_{i,j} \leq 1 - t^{\text{accept}}_{i,j} \quad \forall i \in V^+, j \in V^- \tag{30}$$

$$t^{\text{accept}}_{i,j} \leq 1 - t^{\text{reject}}_{i,j} \quad \forall i \in V^+, j \in V^- \tag{31}$$

$$t^{\text{accept}}_{\text{in},sc_1} = 1 \tag{32}$$

$$\sum\nolimits_{n\in\{m+2,\ldots N_{sc}\}} t^{\text{accept}}_{sc_m,sc_n} = 0 \quad \forall m \in \{1, ..., N_{sc} - 2\} \tag{33}$$

$$\sum\nolimits_{n\in\{m+2,\ldots,N_{sc}\}} t^{\text{reject}}_{sc_m,sc_n} \leq t^{\text{accept}}_{sc_m,sc_{m+1}} \quad \forall m \in \{1, ..., N_{sc} - 2\} \tag{34}$$

$$t^{\lambda}_{i,j} \geq T^{\lambda}_{i,j} \quad \forall i \in V^+, j \in V^-, \lambda \in \Lambda \tag{35}$$

4 Graphical User Interface

A GUI is developed to provide engineers access to the mathematical optimization. To do so, the optimization model has to be adaptable to individual constraints (e.g. existing infrastructure). Furthermore, the GUI should guide the user through all necessary steps in an intuitive way. Since we are dealing with a multi-criteria problem, the performance of different solutions has to be presented in a manner that supports the decision-making process.

The GUI, c.f. Fig. 3, is developed using the MATLAB 2017a App Designer [9]. The tabs on the left side guide the user through the optimization process. In the shown tab, the scope of the optimization (e.g. if the topology is partly given or not) is defined and model details (e.g. limits for the reject rate) are set. To define the objective, weights and limits for the performance indicators are set in another tab. Moreover, it is possible to calculate the pareto front of two objectives. In a last step, solver options are set and the optimization is started.

Once an optimal solution is found, the user can analyze it in detail (e.g. explore optimal topology and operational parameters), or compare different so-

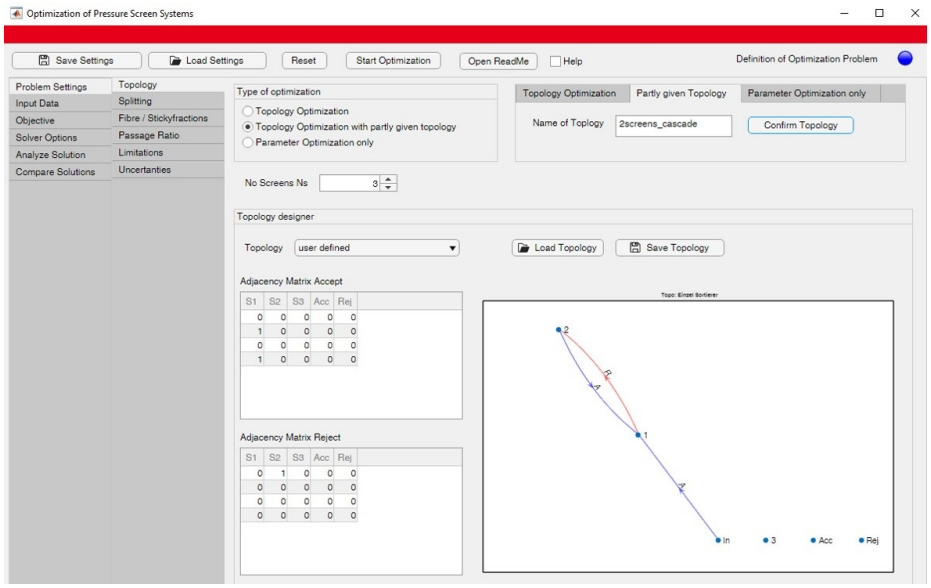

Fig. 3. Basic structure of the GUI.

lutions, cf. Fig. 4. While Pareto fronts are one of the most common methods to visualize a trade-off between objectives, this representation becomes easily confusing when dealing with three or more objectives. [10] gives an overview about different visualization techniques for multi-objective decision making problems. It is pointed out that when choosing a technique, one has to balance information content and clarity. To capture all aspects, it is yet recommended to present the same data in different ways. Thus, to provide a comprehensive overview while at the same time not overloading the user with information, different visualizations of the solutions (Table, Spider Web Plot or Scatter Plot) can be shown up on request. Furthermore, it is possible to display selected solutions and set lower and upper bounds for the visualization. Since an interaction of the decision maker during the generation of pareto-optimal solutions is helpful to understand why a solution is preferred over another and to gain a reasonable trade-off between the objectives [11], the user can simply calculate new solutions (e.g. with different weights) and add them to the plots.

5 Results

In the following, we show an exemplary optimization of a fine screening system with our tool. The underlying optimization model is implemented using MATLAB 2017a with the free toolboxes YALMIP [8] and OPTI [3]. The problem is solved to proven global optimality using SCIP 5.0.1 [6]. The input data are taken from Valkama [15]: $M_{\mathrm{W}}^{\mathrm{input}} = 1936\,m^3/h$, $M_{\mathrm{F}}^{\mathrm{input}} = 28.2\,t/h$, $M_{\mathrm{S}}^{\mathrm{input}} = 1200\,m^2/h$.

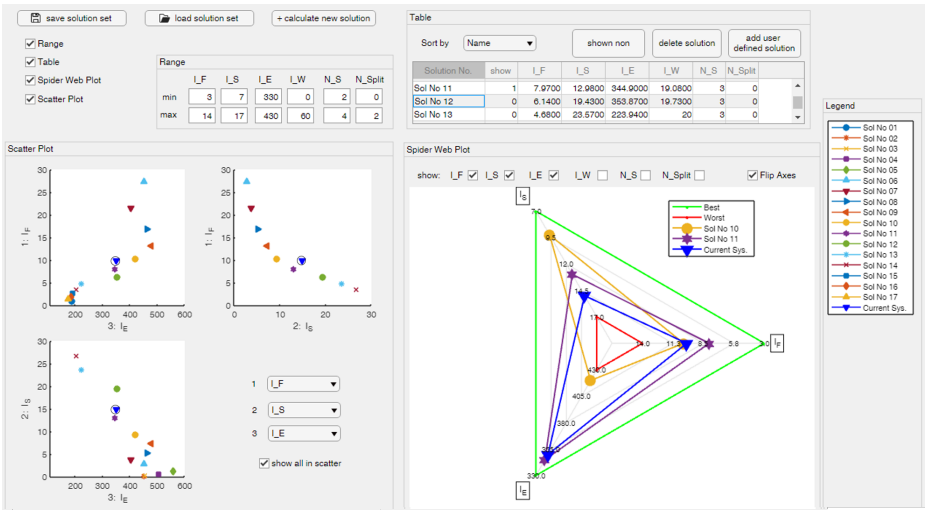

Fig. 4. Tab "Compare Solutions".

The pipe capacity is set to $M_{\mathrm{W}}^{\max} = 4\,M_{\mathrm{W}}^{\mathrm{input}}\,(1 + I_{\mathrm{W}}^{\max})$, $M_{\mathrm{F}}^{\max} = C^{\max}\,M_{\mathrm{W}}^{\max}$ and $M_{\mathrm{S}}^{\max} = 8\,M_{\mathrm{S}}^{\mathrm{input}}$. In total, five designs ($|D| = 5$) are considered with fibre passage ratios $P_{\mathrm{F},d}^{\mathrm{pre}} = \{0.4, 0.525, 0.6, 0.775, 0.9\}$, $d \in D$ and the sticky passage ratios are calculated according to Eq. 4.

To plan a system in practice, one has to adapt the model to individual constraints. In our example, a preexisting system shall be optimized. A part of the existing interconnections should remain and thus we fix a part of the topology by defining $T_{i,j}^{\lambda}$ (cf. panel "Topology designer" in Fig. 3).

The main challenge in a multi-criteria optimization problem is to find a reasonable trade off between the objectives. To reduce complexity, a preselection of objectives and a definition of limits is recommended if possible. We fix the limit of dilution water to $I_{\mathrm{W}}^{\max} = 20\,\%$, and the number of screens to $N_{sc} = 3$. We calculate the pareto front of the key objectives sticky load i_{S} and fibre loss i_{F} with an unbounded energy indicator ($I_{\mathrm{E}}^{\max} = \infty$), c.f. Fig. 5 left. The preexisting non-optimal system is shown as a reference value. Now, a reasonable limit for the fibre loss has to be chosen. Besides the user's individual priority, as a rule of thumb, the gradient of the pareto front at a chosen solution should neither be extremely high nor low since this indicates a saturation of one objective. In our example, we choose a limit of $I_{\mathrm{F}}^{\max} = 8\,\%$ since this yields in a moderate slope and we want to slightly reduce the fibre loss of our current system. In the next step, we calculate the pareto front of sticky load and energy indicator i_{E} with this fixed fibre loss. We notice a step around $i_{\mathrm{E}} = 300\,\%$ (c.f. red arrow in Fig. 5, right). If one prefers low sticky load over low energy consumption, the maximum energy indicator should be set left of the step at $I_{\mathrm{E}}^{\max} = 317\,\%$. Otherwise, a maximum energy indicator of $I_{\mathrm{E}}^{\max} = 187\,\%$ is reasonable since a raise of the energy consumption up to the step decreases the sticky load only slightly.

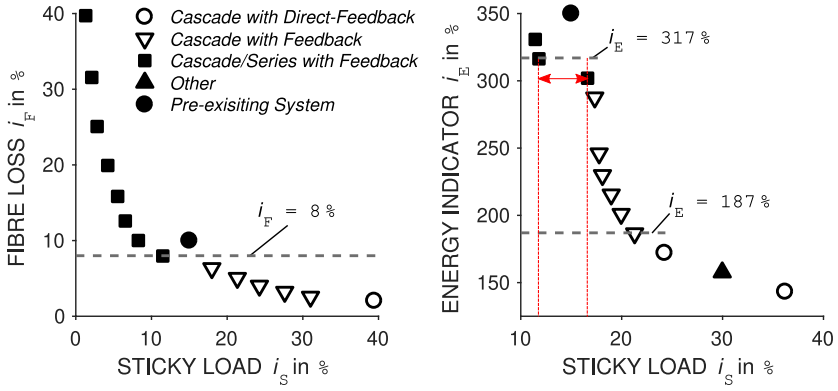

Fig. 5. *Left:* The pareto front of fibre loss and sticky load is used to select a maximum fibre loss $I_{\mathrm{F}}^{\max}$. *Right:* The pareto front of energy indicator and sticky load given a maximum fibre loss of $I_{\mathrm{F}}^{\max} = 8\,\%$ is used to select a maximum energy indicator $I_{\mathrm{E}}^{\max}$.

To investigate the influence of the number of screens on the systems' performance, a spider web plot, c.f. Fig.6, is used. Choosing only two screens results in a significantly higher sticky load and is not recommended even if the energy consumption is lower than the upper bound. In contrast, the sticky load is only slightly reduced for four screens. Thus, three screens appear to be a good trade off. This procedure can be repeated, and e.g. a maximum fibre loss of $I_{\mathrm{F}}^{\max} = 10\,\%$ can be investigated. The resulting options can again be compared in the spider web plot.

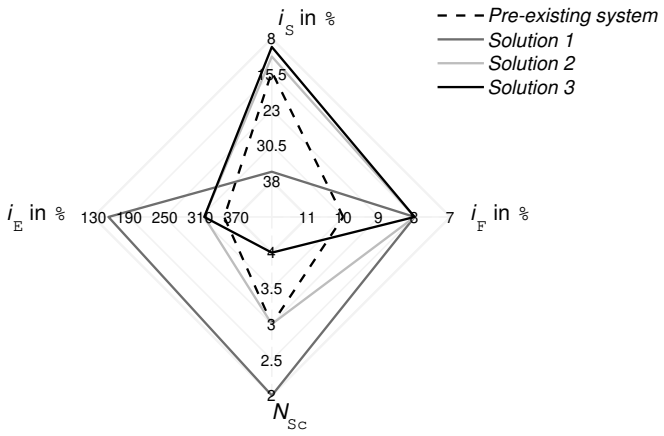

Fig. 6. Spider web plot to investigate the influence of the number of screens N_{sc}. Values further out indicate a better performance.

6 Conclusion

We presented a MINLP for the multi-criteria optimization of pressure screen systems which are used in paper recycling processes. Our approach allows to find the optimal system topology, the optimal selection of suitable screen designs, and optimal operational parameters, and can be easily adapted to other applications in mechanical process engineering. The performance of the pressure screen system is assessed using indicators for fibre loss, contamination load, resource consumption and complexity. To lower the barrier for domain experts who have no or few background in mathematical optimization, we developed a user friendly software tool. The user is guided through the optimization process, and individual conditions can be considered. Also, different solution visualizations are provided to support multi-criteria decision making.

References

[1] Amand, F.: Optimization of stickies removal in screens and cleaners. In: Recent Advances in Paper Recycling - Stickies, pp. 78–125. Wisconsin (2002)
[2] Ämmälä, A., et al.: Effect of design and operational parameters on machine screen pulsation and energy consumption. Nord Pulp Paper Res J **30**(2), 215–219 (2015)
[3] Currie, J., Wilson, D.I.: OPTI: Lowering the barrier between open source optimizers and the industrial MATLAB user. In: Foundations of Computer-Aided Process Operations. Georgia (2012)
[4] Eurostat: Energy balance sheets: 2015 DATA, 2017 edition. Luxembourg (2017)
[5] Fügenschuh, A., Hayn, C., Michaels, D.: Mixed-integer linear methods for layout-optimization of screening systems in recovered paper production. Optim Eng **15**(2), 533–573 (2014)
[6] Gleixner, A., et al.: The SCIP Optimization Suite 5.0. Berlin (2017)
[7] Laurijssen, J., et al.: Paper and biomass for energy? Resour Conserv Recycl **54**(12), 1208–1218 (2010)
[8] Löfberg, J.: YALMIP: A toolbox for modeling and optimization in MATLAB. In: Proceedings of the CACSD 2004
[9] MATLAB: 2017a. The MathWorks, Inc., Natick, Massachusetts, USA
[10] Miettinen, K.: Survey of methods to visualize alternatives in multiple criteria decision making problems. OR Spectrum **36**(1), 3–37 (2014)
[11] Miettinen, K., Ruiz, F., Wierzbicki, A.P.: Introduction to multiobjective optimization: Interactive approaches. In: Multiobjective optimization. Berlin (2008)
[12] Olson, J., Turcotte, S., Gooding, R.W.: Determination of power requirements for solid core pulp screen rotors. Nord Pulp Paper Res J **19**(2), 213–217 (2004)
[13] Schabel, S.: Improvements in screening system configuration using simulation and mill verification. In: 6th Res Forum on Recyc, pp. 79–82. Québec, Canada (2001)
[14] Steenberg, B.: Principles of screening system design: Studies in screening theory I. Sven Papperst **56**(20), 771–778 (1953)
[15] Valkama, J.P.: Optimisation of low consistency fine screening processes in recycled paper production. Doctoral dissertation, TU Darmstadt, Darmstadt (2007)
[16] Verband Deutscher Papierfabriken e.V.: Papier 2017. Bonn (2017)
[17] Wakelin, R.F.: Prediction of fractionation efficiency for pressure screens. Appita J **50**(4), 295–300 (1996)